

# Photochemistry of Alkylindenes in the Gas Phase<sup>1</sup>

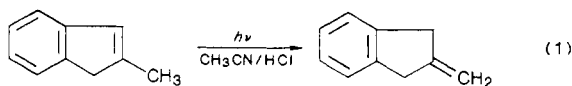
Marie L. Suarez, Robert J. Duguid, and Harry Morrison\*

Contribution from the Department of Chemistry, Purdue University, West Lafayette, Indiana 47907. Received January 6, 1989

**Abstract:** The photochemistry of indene and several alkylindenes has been studied in the gas phase using excitation (254 nm) which populates the S<sub>2</sub> state. Reactions observed in the gas phase involve rearrangements different from those observed in solution, as evidenced by the formation of photoproducts explicable in terms of net hydrogen and alkyl migrations. Photo-dealkylation is also observed at low pressures. In a typical example, gas-phase irradiation of 1-methylindene produces 3-methylindene as the major product, in addition to 2-methylindene, while irradiation in solution leads only to the 2-methyl isomer. The reaction mechanism has been investigated via deuterium-labeling studies, the use of added potential triplet sensitizer and quencher gases, and collisional deactivation by added inert gases. Irradiation of selectively deuterated indenenes results in nearly statistical scrambling in the five-membered ring of the indene skeleton, and multiple 1,5 hydrogen or alkyl migrations are proposed. The lack of triplet sensitization, quenching, or enhancement indicates that the photochemistry is derived from a singlet state. Collisional deactivation results in net quenching of all the photoproducts, with those exclusive to the gas phase quenched at a faster rate than the products observed in solution. Collisional deactivation concomitantly results in an enhancement in fluorescence emission, with little emission observed upon excitation into S<sub>2</sub> in the absence of a quencher gas. A reaction scheme is proposed which involves the generation of photoproducts from S<sub>2</sub> and S<sub>1</sub><sup>vib</sup>.

Although the photochemical properties of many aromatic organic molecules have been extensively and rigorously studied in the gas phase, in most cases the compounds examined have been structurally relatively simple and/or of low molecular weight.<sup>2</sup> Investigations on the photochemistry of substrates of even modest size and complexity have generally been confined to the solution phase, no doubt due, in part, to the requirement of a reasonable vapor pressure to allow for the formation of sufficient quantities of product for characterization. Nevertheless, it is in the gas phase that one has the opportunity to examine the chemistry of upper vibrationally and electronically excited species, because of the reduced deactivation via intermolecular collisions at low pressure, whereas reaction from such states is exceptional when observed in solution.<sup>3</sup> With this in mind, we have initiated a program to explore somewhat larger systems in the gas phase and report herein our observations on the vapor-phase photochemistry of alkylindenes.

Alkylindenes have been studied in dilute solution in some detail in our laboratories, and a photoinduced skeletal rearrangement, involving an interchange of carbon atoms 1 and 2 of the indene skeleton, has been observed in hexane with 254-nm excitation.<sup>4</sup> The mechanism of this transformation is shown in Scheme I. Irradiation in acidic acetonitrile diverts the reaction (cf. eq 1), apparently by protonation of the intermediate bicyclopentene, **1**.<sup>5</sup>



We now report that photolysis of such alkylindenes in the gas phase leads to hydrogen and alkyl rearrangements not hitherto observed in solution. In the Results section, we present (1) the qualitative and quantitative results of the gas-phase photolyses at ca. 1 Torr of 1-, 2-, and 3-methylindenes as well as of 1,1-dimethylindene; (2) studies with deuterated substrates which demonstrate extensive scrambling results from these photolyses; (3) the consequences for both photochemistry and substrate

**Scheme I.** General Mechanism for the Phototransposition of Alkylindenes in Solution

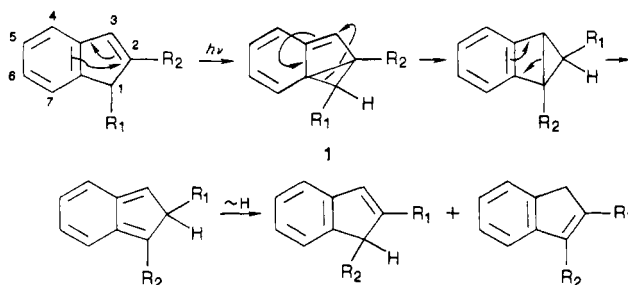


**Table I.** Products and Ratios of the Gas-Phase Irradiation of Various Alkylindenes<sup>a</sup>

starting indene	gas-phase pdts	pdt ratio (% convsn)	soln pdt(s) <sup>b</sup>
1-MI	3-MI/2-MI	3.1 (43) 3.1 (13)	2-MI
2-MI	3-MI/1-MI	2.3 (20) 2.5 (5)	3-MI + 1-MI
3-MI	1-MI/2-MI	2.8 (20) 3.0 (2)	inert
1,1-DMI	2,3-DMI/1,2-DMI/ 1,3-DMI	2.2:1.0:0.56 (24) 2.4:1.0:0.48 (10)	c

<sup>a</sup> "Flowing" conditions; alkylindenes ~0.25 Torr. <sup>b</sup> From ref 4a. <sup>c</sup> No isomeric product detected at 0–10 °C; <sup>3</sup> traces of 1,2-DMI detected at room temperature (this work).

emission of adding "inert" quencher gases to the indenenes; and (4) the effect of excitation wavelength and substrate temperature on the photolyses. We believe the data support a proposal (cf. Figure 9) that the products are derived from upper electronic and vibrational excited states.

## Results

**Gas-Phase Photoproducts of Alkylindenes.** The photoinduced gas-phase rearrangement of 1-methylindene (1-MI) is illustrative of the results obtained with monoalkylindenes. Irradiation of 1-MI with 254-nm light, using either "flowing" or "static" irradiation conditions (cf. Experimental Section; flowing irradiations were typically employed for preparative runs), results in the formation of the two possible isomeric indenenes: 3-methylindene (3-MI) and 2-methylindene (2-MI), both identified by spectral comparison with authentic samples (cf. eq 2). In a similar manner, 2-MI produces a mixture of 1- and 3-MI, and 3-MI gives rise to 1- and 2-MI. Gas-phase irradiation of 1,1-dimethylindene (DMI) similarly results in the formation of all three possible dialkylindenes

(1) Organic Photochemistry. Part 77. Part 76: Mahnken, R. E.; Bina, M.; Deibel, R. M.; Luebke, K.; Morrison, H. *Photochem. Photobiol.* **1989**, *49*, 519–522. Abstracted from the doctoral dissertation of Marie Suarez, Purdue University, Dec 1987. Presented, in part, at the First Winter Conference of the Inter-American Photochemical Society, Jan 3–7, 1988, Clearwater Beach, FL, and the XII IUPAC Symposium on Photochemistry, July 17–22, 1988, Bologna, Italy.

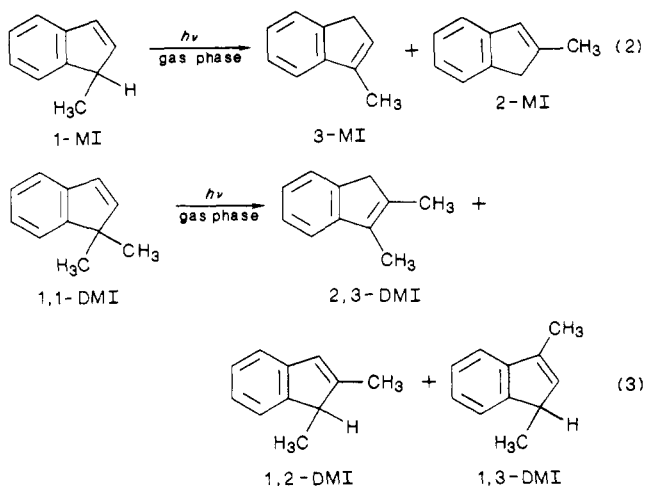
(2) Noyes, W. A., Jr.; Al-Ani, K. E. *Chem. Rev.* **1974**, *74*, 29–43.

(3) Kasha, M. *Discuss. Faraday Soc.* **1950**, *9*, 14–19.

(4) (a) Morrison, H.; Giacherio, D.; Palensky, F. J. *J. Org. Chem.* **1982**, *47*, 1058–1063 and references therein. (b) See also: Padwa, A.; Goldstein, S.; Loza, R.; Pulwer, M. *Ibid.* **1981**, *46*, 1858–1868.

(5) Morrison, H.; Giacherio, D. *J. Org. Chem.* **1982**, *47*, 1058–1063.

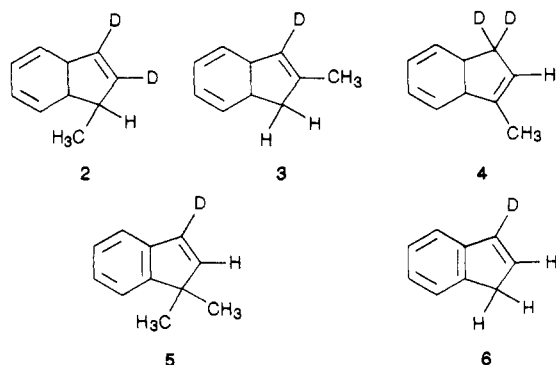
(cf. eq 3). A summary of our data is presented in Table I; in each case, product ratios are presented at two different conversions,



and the relative insensitivity of these ratios to the extent of conversion indicates that we are observing primary photoproducts. The products observed in the solution-phase studies are included for purposes of comparison.

**Quantum Efficiencies of Photoproduct Formation.** These were determined for the monoalkylindenes using static photolysis conditions and the reported<sup>6</sup> gas-phase photochemistry of (*E*)-1-phenyl-2-butene for actinometry and are presented in Table II. Solution-phase data are again included for purposes of comparison.

**Deuterium-Labeling Studies.** Each of the alkylindenes was prepared with deuterium labeling at selected positions on the five-membered ring as shown below (cf. 2–6). The results of



photolyses of these substrates are presented in Table III. All the indenenes show extensive scrambling in the products, and only 1,1-DMI gave unscrambled recovered starting material. That scrambling was independent of conversion to products as was demonstrated by irradiating **2** to a total of 36.1% formation of 2- and 3-MI; the distribution of deuterium in the products was essentially identical with the low conversion data presented in Table III. In a somewhat analogous experiment, **6** was subjected to multiple photolysis/recovery/rephotolysis cycles. The ratios of residual hydrogen at positions 1 and 2 were virtually invariant, i.e., after pass 1 (position 1/position 2), 2.08; pass 2, 2.18; pass 3, 2.08. A 1:1 mixture of 2-MI and its 1,1,3-trideuterio analogue was irradiated as a probe for the possibility of intermolecular exchange. Mass spectral examination of the products gave no evidence of mono- or dideuterated products.

**Collisional Deactivation by Added *n*-Butane.** Irradiation of the three monoalkylindenes and 1,1-DMI with varying pressures of added *n*-butane (static conditions) resulted in extensive quenching

**Table II.** Quantum Efficiencies for the Photorearrangement of Alkylindenes<sup>a</sup>

starting indene	photopdts	$\phi_{\text{product}}$	
		gas phase	soln
1-MI	3-MI	0.3	
	2-MI	0.06	0.029
2-MI	3-MI	0.03	0.023
	1-MI	0.01	0.025
3-MI	1-MI	0.1	
	2-MI	(0.02) <sup>b</sup>	

<sup>a</sup> "Static" conditions; indene pressures ca. 1 Torr; gas-phase values are reported to one significant figure because of the several approximations incorporated in these calculations (see Experimental Section).

<sup>b</sup> Computed by reference to the 1-MI value using the 1-MI/2-MI ratio for the static photolysis of 3-MI.

**Table III.** Hydrogen Distribution after Photolysis of Deuterated Indenes<sup>a</sup>

starting indene	pdts	no. of H's in the 5-C ring		
		C-1	C-2	C-3
<b>2</b>	3-MI (9.7%)	0.73	0.38	
	2-MI (2.7%)	0.74		0.28
	(1-MI) <sup>b</sup>	0.99	0.06	0.03
<b>3</b>	3-MI (6.0%)	1.36	0.68	
	1-MI (2.8%)	0.63	0.53	0.53
	(2-MI) <sup>b</sup>	1.75		0.30
<b>4</b>	1-MI (12.0%)	0.41	0.33	0.33
	2-MI (3.1%)	0.70		0.30
	(3-MI) <sup>b</sup>	0.24	0.77	
<b>5</b>	2,3-DMI (9.5%)	1.0		
	1,2-DMI (6.2%)	0.54		0.47
	1,3-DMI (6.2%)	0.35	0.57	
	(1,1-DMI) <sup>b</sup>		1.0	0
<b>6</b>	indene	1.74	0.82	0.45

<sup>a</sup> "Flowing" conditions. <sup>b</sup> Recovered starting material.

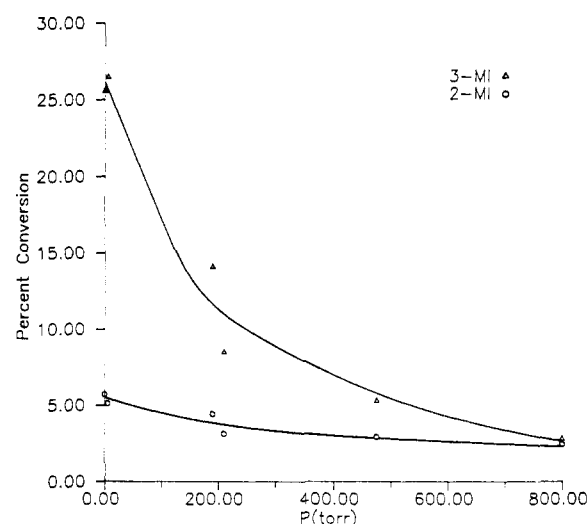


**Figure 1.** Effect of *n*-butane on the photochemistry of 1-MI.

of all of the photoproducts, with those products not seen in solution-phase photolyses typically more completely eliminated. The data are plotted in Figures 1–4; note that for each compound, the photolyses at different butane pressures were carried out under comparable irradiation conditions.<sup>7</sup> It is interesting that, in the photolysis of 2-MI, the 3-MI/1-MI ratio is virtually unaffected by the added butane and remains at ca. 2.6, appreciably different from the value of 0.92 observed in solution.

**Reaction Multiplicity Studies.** Previous studies have demonstrated that the alkylindene skeletal rearrangements in solution derive from the singlet excited state,<sup>4</sup> and several probes were

(6) (a) Comtet, M. *J. Am. Chem. Soc.* **1970**, *92*, 5308–5312. (b) Note that the product ratios in Table II do not directly correlate with the ratios in Table I. The data are consistent with our other static photolyses and we have, in general, found the ratios under static conditions to differ slightly from those obtained in the flowing mode, presumably due to the ca. 4-fold decrease in reactant pressure in the latter case. See also the Discussion section.

(7) We have not, as yet, been successful in uniformly fitting these data to the more obvious (i.e., one- or two-state) mechanistic schemes. Further studies and refinements in the experimental protocol are planned.

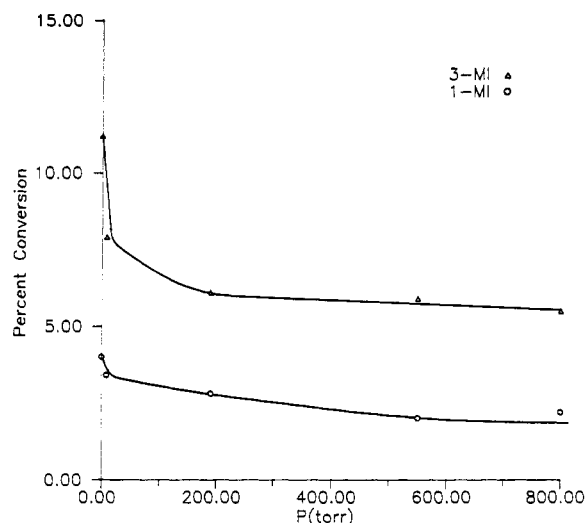


Figure 2. Effect of *n*-butane on the photochemistry of 2-MI.

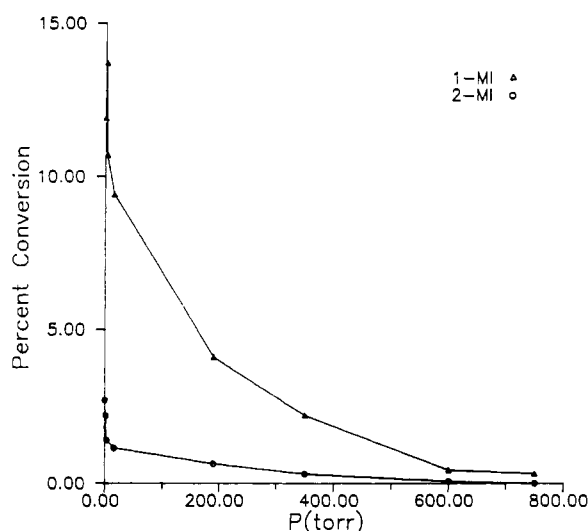


Figure 3. Effect of *n*-butane on the photochemistry of 3-MI.

employed to determine whether the same was true for the gas phase. Acetophenone ( $E_T = 74$  kcal/mol<sup>8</sup>) was used to attempt triplet sensitization of the indenenes ( $E_T = 63$  kcal/mol<sup>9</sup>) using static conditions with 300-nm Rayonet lamps such that acetophenone could be expected to absorb  $> 85\%$  of the incident light. 2-MI and 3-MI, as well as 1,1-DMI, showed decomposition but no evidence for isomerization. 1-MI did form some 3-MI but formed no 2-MI under the sensitization conditions.

1-MI was photolyzed in the presence of varying pressures of added xenon to explore the possible effect of heavy-atom enhancement of intersystem crossing.<sup>10</sup> The data show that, as with butane, there is quenching (though less efficient than with the C<sub>4</sub> hydrocarbon) of both photoproducts. A less extensive experiment with 1,1-DMI also showed that the products are quenched by added xenon. Irradiation of 1-MI with added nitrogen, oxygen, or *cis*-piperylene ( $E_T = 58$  kcal/mol<sup>11</sup>) gave results analogous to those observed with butane and xenon.

**Wavelength Study.** As was noted earlier, all of the above studies were conducted with monochromatic 254-nm light (Rayonet low-pressure mercury lamps) through quartz. The four substrates were also exposed to broad-band light centered at 300 nm using Rayonet lamps and a Pyrex vessel. The photolyses required static

Table IV. Effect of Excitation Wavelength on the Gas-Phase Photochemistry of Alkindenes<sup>a</sup>

starting indene	wavelength, <sup>b</sup> nm	prd ratio	total convsn, %
1-MI	229	3-MI/2-MI	5.3
	254	2.5	31.3
	"300"	4.5	3.9
2-MI	229	3-MI/1-MI	3.3
	254	2.7	15.2
	"300"	2.8	5.5
3-MI	229	1-MI/2-MI	5.2
	254	4.9	14.6
	"300"	4.4	2.0
1,1-DMI	229	2,3-DMI/1,2-DMI/1,3-DMI	14.1
	254	1.9:1.0:0.48	26.8
	"300"	2.2:1.0:0.27	4.3

<sup>a</sup>"Static" photolyses; photolysis times, 229 nm, 4–15 min; 254 nm, ca. 0.3 min; "300" nm, 3–16 h. <sup>b</sup>"300" nm refers to a Rayonet fluorescent bulb, with broad emission centered at 300 nm; the 254- (Hg) and 229-nm (Cd) irradiations employed relatively monochromatic, resonance lamps (see Experimental Section).

Table V. Photolysis of 1-MI at Varying Initial Sample Temperatures<sup>a</sup>

reservoir temp, °C	products, %		
	3-MI	2-MI	indene <sup>b</sup>
25	29.9	9.5	0.74
0	28.9	12.1	2.0
-5	29.3	11.7	3.7
-15	29.3	7.8	6.6

<sup>a</sup>"Flowing" conditions. <sup>b</sup>Identified by GC retention time.

Table VI. Photolysis of 2-MI at Varying Initial Sample Temperatures<sup>a</sup>

reservoir temp, °C	products, %			
	3-MI	1-MI	indene <sup>b</sup>	DMI's <sup>c</sup>
25	10.2	4.4	0.6	
0	15.3	6.0	2.1	4.0
-15	22.6	8.5	8.4	11.8

<sup>a</sup>"Flowing" conditions. <sup>b</sup>Identified by GC retention time. <sup>c</sup>Sum of peaks with retention times corresponding to 1,2-, 1,3- and 2,3-DMI.

Table VII. Photolysis of 3-MI at Varying Initial Sample Temperatures<sup>a</sup>

reservoir temp, °C	products, %		
	1-MI	2-MI	indene <sup>b</sup>
25	13.8	4.7	0.9
0	13.2	9.5	3.3
-5	8.2	11.5	2.0
-15	9.7	9.6	6.7

<sup>a</sup>"Flowing" conditions. <sup>b</sup>Identified by GC retention time.

Table VIII. Photolysis of 1,1-DMI at Varying Initial Sample Temperatures

reservoir temp, °C	products, %			
	2,3-DMI	1,2-DMI	1,3-DMI	MI's <sup>b</sup>
25	12.9	6.2	3.5	
0	18.3	8.7	6.4	1.8
-15	17.5	8.9	13.6	10.1

<sup>a</sup>"Flowing" conditions. <sup>b</sup>Sum of the peaks with retention times corresponding to the three monomethylindenenes.

conditions and extended irradiation times to compensate for the diminished incident intensity and substrate absorbance with such lamps. All of the indenenes underwent photoisomerization to give products identical with those observed using the 254-nm lamps, albeit at somewhat different product ratios. We likewise studied

(8) Murov, S. L. *Handbook of Photochemistry*; Marcel Dekker: New York, 1973; p 3.

(9) Harrigan, E. T.; Hirota, N. *Chem. Phys. Lett.* **1973**, *22*, 29–32.

(10) See, for example: Morrison, H.; Miller, A. *Tetrahedron* **1981**, *37*, 3405–3409, and references therein.

(11) Cf. reference 8, p 5.

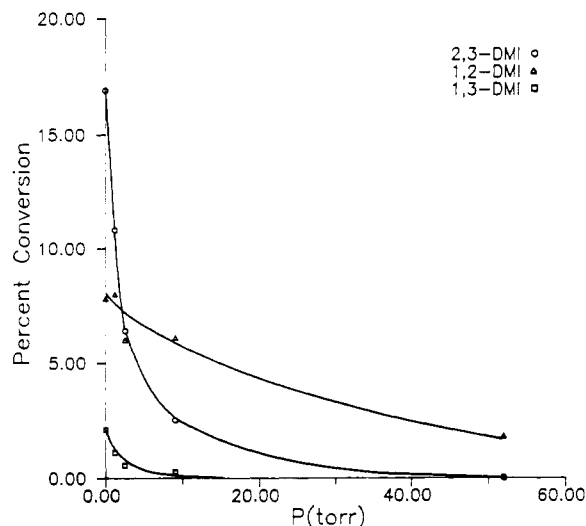


Figure 4. Effect of *n*-butane on the photochemistry of 1,1-DMI.

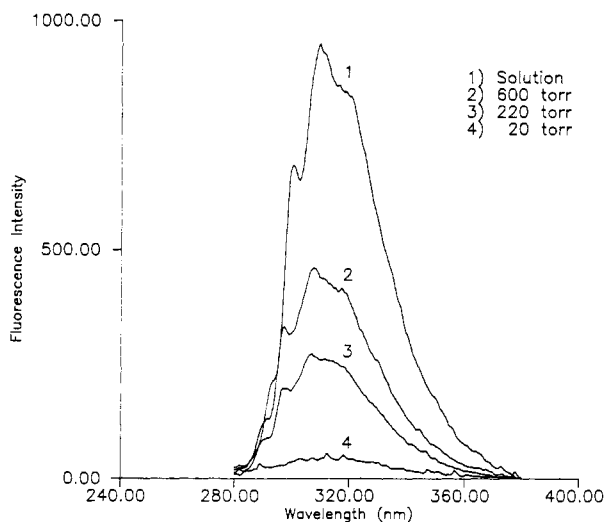


Figure 5. Gas-phase, corrected, fluorescence spectra of 1-MI with varying pressures of *n*-butane by comparison with a  $2 \times 10^{-5}$  M hexane solution of comparable absorbance.

the photolyses of these indenes using the 229-nm resonance line of a cadmium lamp. Again, all products were observed but with yet a different set of ratios. The data are shown in Table IV.

**Photolysis as a Function of Initial Sample Temperature.** The above-described photolyses were carried out with the sample reservoir at room temperature. Studies were also conducted at lower sample temperatures so as to probe the effects of the diminished frequency of molecular collisions expected at reduced pressure (ca. 0.01 Torr) and flow rates. The results are presented in Tables V–VIII. Remarkably, photodealkylation becomes a significant process as the sample temperature is reduced, and in some cases (for example, 2-MI in Table VI), considerable enhancement in conversion results.

**Fluorescence Studies.** By contrast with its modestly efficient fluorescence in solution ( $\phi_f = 0.031^{4a}$ ), 1-MI fluorescence is quite weak in the gas phase.<sup>12</sup> However, the addition of *n*-butane dramatically increases emission (cf. Figure 5).<sup>12</sup> (Similar observations have been made with the other alkylindenes.) The data are presented as fully corrected fluorescence quantum efficiencies in Table IX. Note that, even at the highest pressures of quencher gas, the indene fluorescence efficiency is appreciably below that observed in solution. In Figure 6, we plot both fluorescent enhancement and product quenching by added butane, and it is

Table IX. Quantum Efficiencies for Fluorescence of 1-MI in Solution and in the Gas Phase

butane press, Torr	$\phi_f$	rel $\phi_f$
(hexane)	0.044	1.00
700	0.0082	0.19
600	0.0091	0.21
400	0.0061	0.14
350	0.0051	0.12
220	0.0054	0.12
20	0.0019	0.042

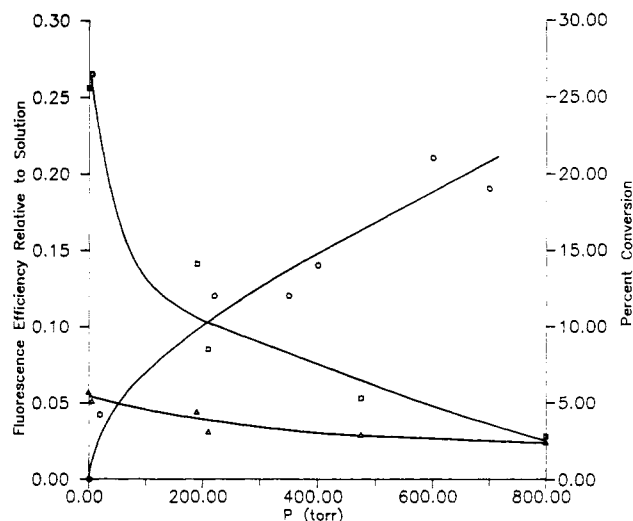


Figure 6. Effect of butane on product formation and fluorescence intensity upon excitation of 1-MI. (O)  $\phi_f$  of 1-MI in the gas phase relative to solution; (□) percent conversion of 1-MI to 3-MI; (Δ) percent conversion of 1-MI to 2-MI.

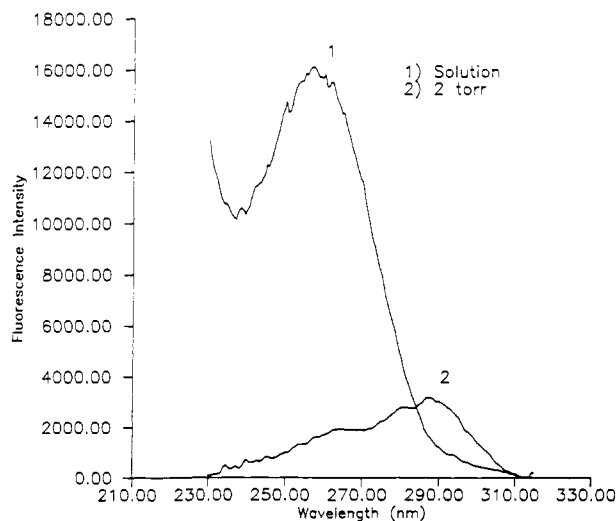


Figure 7. Corrected excitation spectrum for the gas-phase fluorescence of 1,1-DMI.

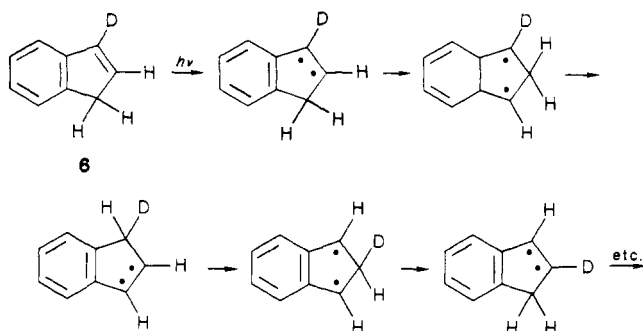
evident that there is appreciable growth in emission at butane pressures well in excess of that needed to eliminate most of the photochemical reaction.

We also studied the effect of excitation wavelength on the fluorescence efficiency of 1,1-DMI. A fully corrected excitation spectrum is presented in Figure 7.

## Discussion

**Nature of the Chemical Reaction(s).** It is clear from the data in Tables I and V–VIII that a number of the products observed upon irradiation of these alkylindenes in the gas phase are not observed upon photolysis in solution. The net structural changes include dealkylation as well as hydrogen and/or methyl rear-

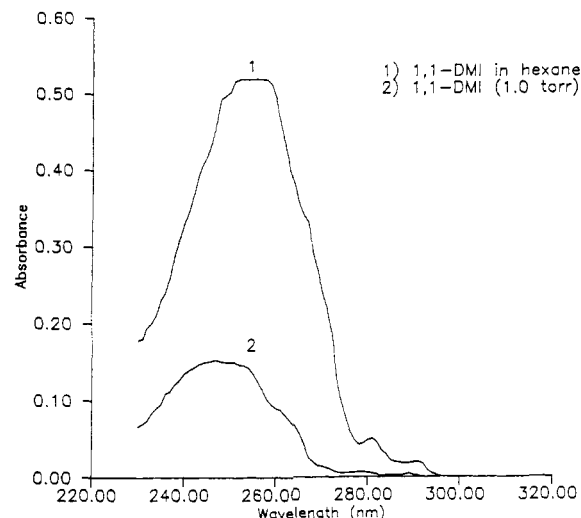
(12) A comparable observation has been made for styrene, cf.: Ghiggino, K. P.; Hara, K.; Mant, G. R.; Phillips, D.; Salisbury, K.; Steer, R. P.; Swords, M. D. *J. Chem. Soc., Perkin Trans. 2* 1978, 88–91, and references therein.

**Scheme II.** Mechanistic Rational for Scrambling of Deuterium in Irradiated 3-Deuterioindene through a Series of 1,5 Hydrogen/Deuterium Shifts

rangements, with some of the latter potentially explicable by the skeletal reorganization mechanism previously observed in solution (see Scheme I). However, the fact that all possible (five-membered ring substituted) isomers are formed from each of the mono-alkylindenes, as well as from 1,1-DMI, suggests that whatever products the solution and gas-phase photolyses have in common may be superficial and that the mechanism in Scheme I may well not be operative in the gas phase. Rather, it appears as if the hydrogen and alkyl groups are capable of migrating to each of the three potential five-membered sites of the indene skeleton.

This conclusion is supported by the deuterium-labeling studies, for extensive (virtually statistical) scrambling into all possible positions was observed in each of the cases examined (cf. Table III), and the labeling patterns are not readily rationalized by the obvious alternative mechanistic possibilities. A prototypical example is 2,3-dideuterio-1-methylindene (2). Though a combination of 1,3 and/or 1,5 hydrogen shifts plus the skeletal rearrangement mechanism could, in principal, generate the 2- and 3-methylindene products formed by 1-MI, a detailed analysis of the scrambling pattern confirms that no combination of these pathways could give the scrambling observed.<sup>13</sup> Likewise, one cannot readily explain the formation of 2-deuterioindene from 3-deuterioindene (6) nor 2-deuterio-1,3-dimethylindene from 3-deuterio-1,1-dimethylindene (5). Nevertheless, intermolecular scrambling was ruled out by irradiating a mixture of 1,1,3-trideuterio-2-methylindene and undeuterated 2-MI (no mono- or dideuterated products observed). Thus, it appears that the excited species can generate a virtually equilibrated mixture of products, presumably by exploring multiple binding sites, a suggestion supported by the sequential photolysis of 6, which showed, after each pass, a statistical distribution of H at C-1 and C-2.

One mechanistic picture, in terms of valence bond structures, which could account for the scrambling of hydrogen and/or alkyl groups in the photoproducts, would be multiple, sequential 1,5 shifts via diradical intermediates in the excited state.<sup>14</sup> This proposal is illustrated in Scheme II for 3-deuterioindene. It is evident from the quantum efficiencies presented in Table II that hydrogen shifts are 5–10-fold more efficient than alkyl migrations, the latter having values comparable to those observed in solution. Note that hydrogen shifts are actually occurring with far more efficiency than the quantum yield data indicate, as evidenced by the significant scrambling of starting material seen in Table III. A useful example is 2-MI, in which the hydrogen shift is a degenerate process. The ca. 30% scrambling of D from C-1 to C-3, relative to the 9% methyl shift product (Table III), indicates that hydrogen migration occurs with a quantum efficiency of 0.1 (a

**Figure 8.** Absorption spectra of 1,1-DMI in the gas phase and as a  $1.0 \times 10^{-4}$  M solution in hexane.

value comparable to that seen for conversion of 3-MI to 1-MI). Clearly, diradicals are unlikely to exist as such, and an alternative picture would have the hydrogen and alkyl groups within the highly energetic excited species exploring the energy surfaces for migration at levels well above the potential energy barriers associated with such shifts. Collisionally induced decay would then funnel the rearranged molecule back to the product ground state.

It is also noteworthy that the dealkylation products observed in the low-temperature experiments (Tables V–VIII) can be rationalized as resulting from homolytic cleavage of the diradicals in Scheme II. The intent of these experiments was to probe the photochemical consequences of lowered substrate vapor pressure (and thus diminished molecular collisions) in the photolysis vessel. Such conditions may be expected to maximize vibrational excitation and facilitate homolysis (see also below).<sup>15</sup>

**Collisional Deactivation Studies and the Nature of the Reacting State.** Two electronic transitions are in the solution- or gas-phase UV absorption spectra of indenenes (for example, see Figure 8). In indene itself, the lowest energy band ( $S_1$ ) has a  $\lambda_{\max}$  at 280 nm. This is a forbidden transition, related to the  $L_b$  transition in benzene, and has a low oscillator strength ( $f = 0.003$ ).<sup>16,17</sup> The higher energy band ( $S_2$ ), with a  $\lambda_{\max}$  in indene at 250 nm and an oscillator strength of 0.19, is related to the  $L_a$  transition of benzene.<sup>15,16</sup> It is difficult to distinguish the two transitions in the absorption spectra because of the low intensity of the  $L_b$  band, but the lack of emission from the  $S_2$  state (see below) allows the  $S_1$  transition to be readily discerned (see Figure 7). The mercury resonance line (253.7 nm) used in most of our gas- and solution-phase studies would therefore initially populate  $S_2$ .

There is good photochemical and photophysical evidence to assign the skeletal rearrangements in solution to excited singlet precursors, and both precedent and the data would suggest that these are the lowest vibrational levels of  $S_1$  (i.e., primarily  $S_1^0$ ).<sup>4a</sup> Such rapid decay of upper electronically and vibrationally excited states in solution is to be expected. The generally negative results we have obtained in the gas phase with triplet quenchers and sensitizers, as well as with the heavy-atom reagent, xenon, imply that a singlet excited state is also involved in this chemistry.

(13) For example, a 1,3 H shift gives 3-MI with H exclusively at C-1, yet the product contains H at C-2. This would appear to require a contribution from a pair of sequential 1,5 H shifts, which should also, in part, regenerate 1-MI with H only redistributed into C-2. In fact, the recovered starting material has an equivalent amount of H at C-3. Furthermore, the 2-MI product has a virtually statistical distribution of H at C-1 and C-3 (2.2:1.0), whereas skeletal rearrangement only places H at C-1.

(14) Photoinduced 1,5 aryl shifts have been observed in solution,<sup>4b</sup> as have net 1,3 hydrogen shifts in 1-arylindenes<sup>4b</sup> and *n,m*-dialkylindenes;<sup>4a</sup> the latter have not been studied in depth.

(15) In one case (2-MI, Table VI), there is evidence for a methyl-transfer reaction to form DMI's. We are considering the possibility of condensation in the reaction vessel and consequent wall effects, but a definitive rationale must await further study. Secondary photochemistry as a potential source of dealkylation is also being investigated.

(16) Evleth, E. M. *Theoret. Chim. Acta* 1970, 16, 22–32. See also: Ziegler, L. D.; Varotsis, C. *Chem. Phys. Lett.* 1986, 123, 175–181, and references therein.

(17) There has as yet been no definitive identification of Rydberg transitions in indenenes; cf.: Duncan, A.B.F. *Rydberg Series in Atoms and Molecules*; Academic Press: New York, 1971. Byrne, J. P.; Ross, I. G. *Aust. J. Chem.* 1971, 24, 1107–1141.

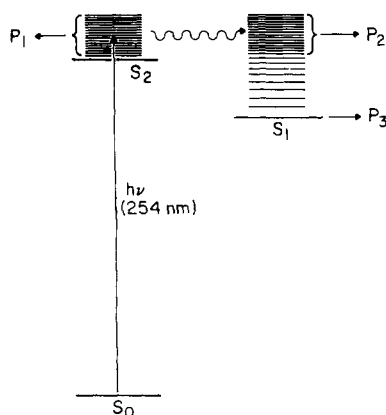


**Figure 9.** Energy level diagram illustrating the proposed origin of the various indene photochemical reaction products.  $P_1$  represents dealkylation products,  $P_2$  represents alkyl and hydrogen shift products, and  $P_3$  represents skeletal rearrangement products.

However, the distinctly different gas-phase chemistry requires that the reactive species to be different from that active in solution. These species could include  $S_2$  (possibly vibrationally excited, i.e.,  $S_2^{\text{vib}}$ ),  $S_1^{\text{vib}}$ , or  $S_0^{\text{vib}}$ .

Any of the above could, in theory, be responsible for the chemistry being observed under our conditions, and all could be expected to be collisionally deactivated by added gases. For example, 254-nm excitation of 1-phenyl-2-butene produces *E/Z* isomerization in solution, but in the gas phase, such irradiation generates both olefin isomerization and a di- $\pi$ -methane reaction to 1-phenyl-2-methylcyclopropane.<sup>6</sup> *n*-Butane selectively quenches the latter product, and collisional deactivation of vibrational levels of a  $T_2^{\text{vib}}$  precursor to the cyclopropane is proposed. The photoisomerization of fulvene to benzene with 254-nm excitation is likewise quenched by isopentane, and the reaction is attributed to  $S_2^{\text{vib}}$ .<sup>18a</sup> Ethane has been used as a quencher gas to study the photocarbonylation of benzaldehyde, the chemistry being attributed to  $T_2^{\text{vib}}$  and  $T_1^{\text{vib}}$ .<sup>18b</sup> It is generally accepted that collisional deactivation of vibrational excitation is more efficient than the analogous quenching of electronic excitation,<sup>19,20</sup> though this may be less true for  $S_2$  than for  $S_1$ .

The observations in this study that are critical to a mechanistic discussion are (1) the appearance of photoproducts analogous to those seen in solution together with products unique to the gas phase; (2) the quenching, in whole or in part, of all of these products by inert gases; (3) the differential character of this quenching, with limited and less efficient quenching of the products seen in solution, compared with continuous, more efficient, and, in two cases (3-MI, 1,1-DMI), complete quenching of products unique to the gas phase; (4) the absence of emission upon excitation into  $S_2$ ; but (5) the simultaneous induction of fluorescence concomitant with the quenching of reaction by inert gases, the former continuing to occur at butane pressure well beyond that needed to eliminate most of the photochemical reaction. Also worth noting is the fact that hydrogen<sup>21a</sup> (as well as vinyl<sup>21b</sup> and aryl<sup>21a</sup>) shifts have been observed in the thermochemistry of indenenes but there are no such reports for alkyl shifts.<sup>21c</sup>

We believe the best rationale of the above data is a cascade mechanism (Figure 9) for the gas-phase photoproducts, with

dealkylation possibly originating from  $S_2$  (or a species derived therefrom) and the hydrogen and alkyl shifts primarily originating from  $S_1^{\text{vib}}$ . The excitation spectrum in Figure 7 nicely demonstrates that radiationless paths compete effectively with emission from  $S_2$ . As collisional quenching of  $S_2$  occurs, upper and eventually lower vibration levels of  $S_1$  become populated so that photochemistry (and emission) characteristic of the solution phase become observable,<sup>22</sup> while products unique to the gas phase are virtually eliminated. The vibrationally activated  $S_1$  state should have more than sufficient energy to explore the reaction surfaces associated with the valence bond picture in Scheme II, before adventitious collisions deactivate the species into one of the isomer potential energy wells.<sup>23–26</sup>

## Conclusions

Monoalkylindenes show distinctly different photochemistry in the gas phase from that observed in solution, though there is evidence that the chemistry originates within the singlet manifold in both media. It is proposed that reactions in the gas phase derive from  $S_2$  and  $S_1^{\text{vib}}$ , with the latter giving rise to a novel scrambling of substituents about the five-membered ring via sequential 1,5 shifts. Clearly the indene system presents a fertile area for detailed photophysical studies involving single vibronic level excitation, and collaborative efforts in this direction are planned. An extension of our gas-phase photochemical studies to the homologous 1,2-dihydronaphthalenes is also in progress, and chemistry analogous to that described above is already evident.

## Experimental Section

The detailed experimental procedures for this work may be found in the doctoral dissertation of M.L.S. The salient features are summarized below.

**Materials.** Nitrogen and oxygen, from Airco, were dried by passing through Drierite prior to use. Tetrahydrofuran and ethyl ether were distilled under nitrogen from sodium benzophenone. Benzene was distilled under nitrogen from sodium. All other reagents were used as received. 2,3-Dideuterio-1-methylindene (**2**) was prepared by potassium carbonate catalyzed deuteration of 3-methyl-1-indanone, followed by reduction with  $\text{LiAlD}_4$  and dehydration with deuterated *p*-toluenesulfonic acid. 3-Deuterio-2-methylindene (**3**) was prepared by reduction of 2-methyl-1-indanone with  $\text{LiAlD}_4$  followed by dehydration. 1,1-Dideuterio-3-methylindene (**4**) was prepared by sodium methoxide catalyzed exchange of 3-methylindene with  $\text{D}_2\text{O}$ . 3-Deuterio-1,1-dimethylindene (**5**) was prepared by reduction of 3,3-dimethyl-1-indanone with  $\text{LiAlD}_4$  followed by dehydration. 3-Deuterioindene (**6**) was prepared by reduction of 1-indanone with  $\text{LiAlD}_4$  followed by dehydration.

**Gas Chromatography.** Preparative gas chromatography was performed on a Varian Model 90P instrument equipped with a thermal conductivity detector, and connected to a Leeds and Northrup Speedo-

(22) We would expect that the mechanism of, for example, the alkyl shifts seen with 2-MI might well change from the multiple substituent migration proposed in Scheme II to the skeletal reorganization demonstrated for the solution phase (Scheme I). An appropriately labeled substrate is being prepared to test this hypothesis.

(23) The Arrhenius activation energies for the thermal 1,5 shifts of a vinyl or aryl group are ca. 33 kcal/mol,<sup>21</sup> while the computed free energy of activation associated with a 1,5 H shift is ca. 39 kcal/mol.<sup>24</sup> There are no equivalent data for the photochemical rearrangements. It is interesting to note that the energy gap between  $S_1^0$  and  $S_2^0$  can be estimated at ca. 9 kcal/mol (calculated from the spectra in ref 16 and assuming that the 0,0 transitions are at 294 and 270 nm, respectively). Excitation with 254-nm light creates  $S_2^{\text{vib}}$  with ca. 16 kcal/mol excess energy relative to  $S_1^0$ .

(24) Roth, W. R. *Tetrahedron Lett.* **1964**, 1009–1013.

(25) The barriers associated with hydrogen shifts can be expected to be appreciably lower than those corresponding to alkyl shifts. This could explain the increased amount of alkyl shift seen from 1-MI with higher frequency excitation (see Table IV). However, we cannot explain why an analogous increase in the relative amount of alkyl shift product is not also observed for 3-MI.

(26) Deuterium scrambling should also be maximized in  $S_1^{\text{vib}}$  and therefore reduced by added butane. This is a difficult prediction to confirm because of the reduced conversion in the presence of the quencher gas. However, multiple photolyses of 2,3-dideuterio-1-methylindene (**2**) in the presence of 90–130 Torr of butane pressure did allow for the accumulation of sufficient 2- and 3-MI to permit NMR analysis. Both compounds showed some reduction in scrambling, with the effect most evident in 2-MI, where the C-1 and C-3 hydrogen content was 0.85 and 0.15, respectively. These numbers were 0.74 and 0.28 without added butane (cf. Table III). Note that the trend is consistent with an increasing role for the solution-phase (skeletal reorganization) mechanism, which places H exclusively at C-1.

(18) (a) Kent, J. E.; Harman, P. J.; O'Dwyer, M. F. *J. Phys. Chem.* **1981**, *85*, 2726–2730. (b) Berger, M.; Goldblatt, I. L.; Steel, C. *J. Am. Chem. Soc.* **1973**, *95*, 1717–1725.

(19) For example, the efficiency for electronic quenching of formaldehyde  $S_1$  by butane is only 0.002, whereas vibrational quenching of the same state proceeds with virtually unit efficiency; cf.: Shibuya, K.; Lee, E. K. C. *J. Chem. Phys.* **1978**, *69*, 758–766.

(20) Wayne, R. P. *Photochemistry*; American Elsevier: New York, 1970; p 97.

(21) (a) Miller, L. L.; Boyer, R. F. *J. Am. Chem. Soc.* **1971**, *91*, 650–656, and references therein. (b) Field, D. J.; Jones, D. W. *J. Chem. Soc., Chem. Commun.* **1977**, 688–690. (c) An excellent review and discussion of simple olefin photochemistry in terms of electronic excited versus hot ground states may be found in: Collin, G. J. *Adv. Photochem.* **1988**, *14*, 135–177.

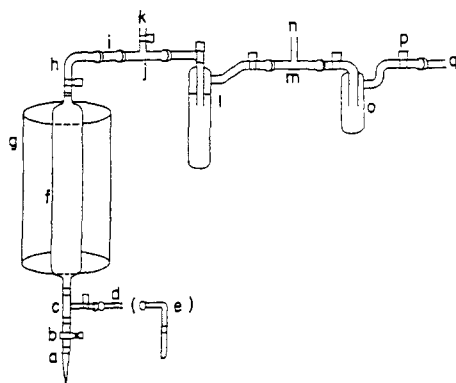


Figure 10. Gas-phase photolysis apparatus.

max H recorder. Columns with outer diameter of 0.25 in. were used with helium as a carrier gas for preparative work. Analytical work was performed on two instruments, each equipped with a flame ionization detector. A Hewlett-Packard Model 5170A instrument was used with a 0.25-mm inside diameter capillary column. It was operated with nitrogen, hydrogen, and air flow rates of 30, 30, and 240 mL/min, respectively. A Hewlett-Packard Model 3390A integrator was used with this chromatograph. The second analytical instrument was a Varian Series 1400 chromatograph, used with 0.125-in. outside diameter columns. It was operated with nitrogen, hydrogen, and air flow rates of 30, 30, and 220 mL/min, respectively, and used with a Hewlett-Packard Model 3380S integrator.

**Columns.** The following columns were used in this study: A, 30-m  $\times$  0.25-mm i.d., Superox, capillary, 0.25- $\mu$ m film thickness; B, 15 ft  $\times$  0.125 in., 10% XF-1150 on 60/80 AW-DMCS Chromosorb W; C, 18 ft  $\times$  0.25 in., 25% XF-1150 on 60/80 AW Chromosorb P, 70 mL of He/min; D, 20 ft  $\times$  0.25 in., 15% XF-1150 on 60/80 AW Chromosorb W, 60 mL of He/min; E, 20 ft  $\times$  0.25 in., 30% SF-96 on 60/80 AW DMCS Chromosorb W, 60 mL of He/min.

Typical conditions and retention times (in minutes) were as follows: column A at 80  $^{\circ}$ C, 1-MI (19.4), 2-MI (35.0), 3-MI (32.2); column B at 140  $^{\circ}$ C, 1-MI (10.8), 2-MI (17.8), 3-MI (14.7), 1,3-DMI (12.7), 1,2-DMI (15.9), 2,3-DMI (22.6). Preparative GC in the monoalkylindene series utilized column C at temperatures of 135–160  $^{\circ}$ C. Preparative GC for the dialkylindenes utilized column C or D at 130  $^{\circ}$ C. (E)-1-Phenyl-2-butene was purified by column E at 115  $^{\circ}$ C. The E and Z isomers and the cyclopropane product reported by Comtet<sup>6a</sup> were assayed on column A at 70  $^{\circ}$ C with retention times of 17.8, 19.8, and 20.4 min, respectively.

**Spectroscopy.** Routine proton spectra were recorded on a 90-MHz Perkin-Elmer R-32 instrument. For more accurate and precise analyses or when the amounts of sample were limited, a Varian Model XL-200 or a 470-MHz Nicolet instrument was used. In order to allow long enough relaxation times for all the vinyl protons of alkylindenes when the high-field instruments were used, it was found necessary to allow a delay time between pulses longer than the default value of 3 s. Usually, a value of 30 sec was used.

Ultraviolet spectra were recorded on a Cary 17D spectrophotometer. Single-wavelength absorbance measurements were made on a Gilford modified Beckman DU instrument. All measurements were made using 1-cm path length quartz cells. For gas-phase measurements, the cell used in the fluorescence studies was employed.

Mass spectra were recorded at the Purdue Chemistry Department Mass Spectrometry Center on a Finnigan 4000 mass spectrometer (source temperature of 250  $^{\circ}$ C) with GC capabilities.

Fluorescence spectra were recorded on a previously described<sup>27</sup> right-angle-recording spectrofluorometer now equipped with microcomputer data handling and analysis.<sup>28</sup> Spectra were recorded using a 1-cm square fluorescence cell from Wilmad Glass Co., to which a Teflon high-vacuum valve (0–4-mm bore, available from Kontes) was attached.

**Photochemical Apparatus.** The photochemical apparatus used in the gas-phase photochemistry studies consisted of a photolysis vessel surrounded by 16 Rayonet lamps and connected to a vacuum line (cf. Figure 10). The compound to be photolyzed was placed in a V-shaped flask, a, which was connected to b, an adapter containing a high-vacuum Teflon valve. Component b allowed convenient degassing of the sample. Addition of gases or liquids to the system was achieved with the T-shaped

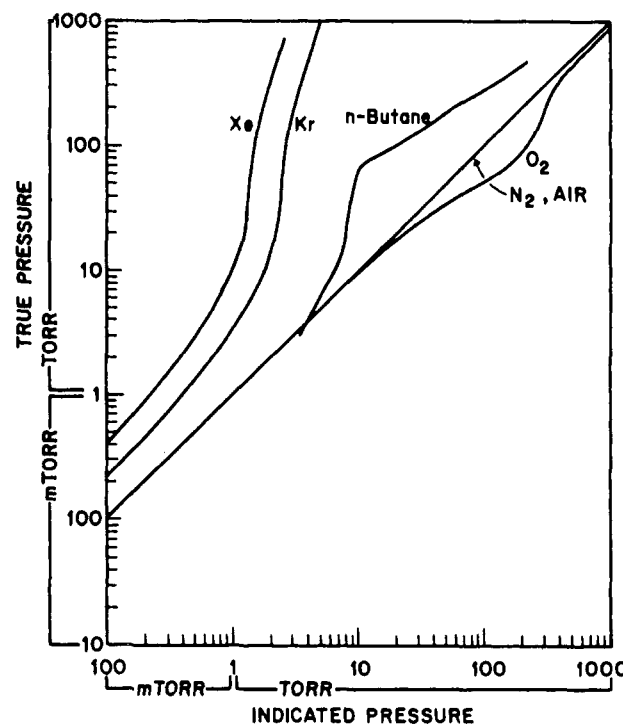


Figure 11. Calibration curves for the Granville-Phillips vacuum gauge.

adapter, c. A high-vacuum Teflon valve on the side arm allowed for the isolation of the photolysis system from the gas or liquid being added. When gases were added, d was connected to vacuum tubing, which in turn was connected to the regulator or control valve of the gas cylinder. In the case of the addition of liquids, component e was used, which consisted of an L-shaped tube attached to the flask containing the liquid. The photolysis vessel, f, was a quartz or Pyrex tube, 33–35 cm in length  $\times$  14.5–15.5 cm in circumference, which was placed inside the photochemical reactor, g. Connected to the photolysis vessel was adapter h, containing a high-vacuum Teflon valve, which served to isolate the vessel from the rest of the vacuum line. This was joined to i, which served as a flexible connection between the more rigid horizontal part of the vacuum line (components j–p) and the vertical part of the line (components a–h). T-shaped adapter j was connected to the first vacuum gauge, k, via a Cajon Ultra-Torr Union (1/2-in. tube o.d.). This gauge was a Granville-Phillips (GP) Series 275 convection vacuum gauge with analog readout in Torr and mTorr. It had a useful measuring range from 1 mTorr to 1000 Torr of nitrogen or air pressure. This gauge could be isolated from the rest of the system by a high-vacuum Teflon valve on component j. The first cold trap, l, was used with liquid nitrogen and was used to trap the photolyzed sample. This was a Kontes vacuum trap, which contained high-vacuum Teflon valves at the entrance and exit. The second vacuum gauge, n, was connected to the system via adapter m with a Cajon Ultra-Torr Union. This was a Pirani vacuum gauge, Type GP-110, available from Consolidated Vacuum Corporation. It had a measuring range from 1 mTorr to 2 Torr of air pressure. The second cold trap, o, was also used with liquid nitrogen and was used as a safety measure to protect the vacuum pump from impurities. It contained high-vacuum Teflon valves at the entrance and exit. Adapter p served to connect the cold trap to high-vacuum rubber tubing which was in turn attached to the vacuum pump, q. Either a Duo Seal or a Wegner vacuum pump was used. All samples were deoxygenated by freeze–pump–thaw cycles prior to irradiation.

The photochemical reactor was made from components of a Model RPR-100 Rayonet reactor, available from Southern New England Ultraviolet Company. It consisted of a cylindrical-shaped reflective metal surface on which 16 photochemical lamps were connected. Rayonet lamps, available from Southern New England Ultraviolet Company, were used. Except as noted, photolyses employed 16 254-nm lamps. The 299-nm irradiations were performed with a Phillips cadmium lamp with a glass envelope and quartz burner, with a 0.9-A operating current. This lamp was connected to an Ealing universal spectral lamp power supply. During photochemical studies, the lamp was placed inside the metal housing of the reactor.

**Calibration of the Granville-Phillips Vacuum Gauge.** The GP Series 275, a thermal conductivity gauge (k in Figure 10), was used to monitor the pressure of the compound to be photolyzed under static conditions and to measure the pressure of added gases. This gauge is calibrated for

(27) Brainard, R.; Morrison, H. *J. Am. Chem. Soc.* **1971**, *93*, 2685–2692.

(28) We are grateful to Dr. Gary Kramer and Daniel Severance for their assistance in modifying the fluorimeter.

nitrogen or air, and conversion curves were needed when other gases were used. Of the gases used in this work, a calibration curve was available from Granville-Phillips only for oxygen (see Figure 11). A calibration curve was constructed for *n*-butane by measuring the vapor pressure of liquid butane at different temperatures of a slush bath, employing the equation

$$\log P \text{ (torr)} = (-0.05223/T)A + B$$

where  $A = 23450$  and  $B = 7.395$  for butane at temperatures from  $-100$  to  $+12$  °C. For xenon, an indicated pressure on the GP gauge of approximately 2.2 Torr was determined to correspond to atmospheric pressure. No other calibration points were available for xenon, but a curve for krypton, in which 4.5 Torr corresponds to atmospheric pressure, was reported in the GP gauge instruction manual. Xenon was assumed to have a similarly shaped curve, but went from 2.2 rather than 4.5 Torr on the indicated pressure scale (see Figure 11). The apparent pressures of the alkylindenes in the static photolyses were also corrected, by actual measurement of the mass of "1 Torr" of 1-MI and assuming ideality of the vapor. The correction (1 Torr on the gauge = 0.67 Torr of "true" pressure) was then extrapolated to the other indenes and also assumed to be generally applicable for all low-pressure measurements in the indene series.

**Quantum Efficiencies.** These were carried out using, as a secondary actinometer, the reported<sup>6</sup> quantum efficiencies of 0.075 and 0.066, respectively, for ca. 254-nm photoisomerization of (*E*)-1-phenyl-2-butene to the *Z* isomer and cyclopropane product. Absorbance values for the

actinometer and the indenes were measured in a 1-cm rectangular cell and extrapolated by the Beer-Lambert law to the cylindrical reaction vessel, after correction of the path length by the expression  $L = \pi d/4$ . The fraction of incident light absorbed by 1-phenyl-2-butene was quite low (3.1%) but was ca. 60% for the indenes. The experiments were typically at ca. 1 Torr, with the absolute amount of the indenes determined after correction for gauge response (see above). The amounts of the photoproducts formed were determined relative to unreacted starting material by multiple GLC analyses using column A. Light intensities were typically of the order of  $(3.4\text{--}3.8) \times 10^{17}$  photons/s.

**Photolyses.** In flowing analytical runs, the sample (5–15 mg) was degassed at 0.02–0.05 Torr and then photolyzed by flowing through the vessel ( $T$  ca. 42 °C) using lamps that had been warmed up for 15 min. Typically, the pressure before the collection trap was 0.2–0.3 Torr, and the photolyses took about 1 min. Flowing preparative runs employed batches of 25–30 mg of sample, with cleaning of the quartz reaction vessel between each run to remove polymer. (The cleaning procedure utilized rinsing by acetone, hexane, acetone, and methanol; periodically a thorough baking in a glass-blower's annealing oven was required to eliminate polymer and color.) The mass recovery after photolysis was usually 75–85%. Static photolyses were carried out in an analogous fashion but with the sample constrained to the reaction vessel at the desired pressure.

**Acknowledgment.** We are grateful to the National Science Foundation (Grant CHE-8700333) for support of this research.

## Association Dimers, Excimers, and Inclusion Complexes of Pyrene-Appended $\gamma$ -Cyclodextrins

Akihiko Ueno,\* Iwao Suzuki, and Tetsuo Osa

Contribution from the Pharmaceutical Institute, Tohoku University, Aobayama, Sendai 980, Japan. Received January 17, 1989

**Abstract:** Pyrene-appended  $\gamma$ -cyclodextrins (**1–4**) were synthesized in order to substantiate the 2:2 pyrene- $\gamma$ -cyclodextrin complex as well as to determine the factors that govern their host–host and host–guest association phenomena. The absorption, circular dichroism, and fluorescence spectra of these compounds measured in 10% dimethyl sulfoxide aqueous solutions exhibit spectral characteristics of the pyrene pendant, which reflect such association phenomena. The pyrene moiety of **1** and **2** was connected with the primary hydroxyl group of  $\gamma$ -cyclodextrin through amide (**1**) and ester (**2**) bonds, but that of **3** and **4** was connected with the secondary hydroxyl groups at C<sub>2</sub> and C<sub>3</sub>, respectively, through ester bonds. The  $\beta$ -cyclodextrin derivative **5**, which has a pyrene moiety connected to the primary hydroxyl group through an ester bond, was also synthesized for comparison. Compounds **1** and **2** accommodate the pyrene moiety into their own cavities, forming intramolecular inclusion complexes, which then convert into dimers with the association constants of  $1.74 \times 10^5$  and  $1.53 \times 10^4 \text{ M}^{-1}$  for **1** and **2**, respectively. However, the pyrene moiety of **3** and **4** is not deeply inserted into the cavity, resulting in the limited formation of such association dimers. The results support the reported conclusion that the 2:2 pyrene- $\gamma$ -cyclodextrin complex is formed by dimerization of the 1:1 complex. The fluorescence spectra of **1–5** exhibit patterns reflecting the equilibrium between monomer and association dimer with the order of excimer to monomer intensity ratio of  $5 < 4 < 3 < 2 < 1$ . The observation that the ratio of **1** dropped around pH 12.5 with increasing pH led to the conclusion that in the association dimer two  $\gamma$ -cyclodextrin units are joined together with the secondary hydroxyl group sides facing each other. The excited pyrene moiety of **1** and **2** is remarkably protected against quenching, contrasting to the small degrees of protection of **3** and **4**. Furthermore, the pyrene excimers formed in the association dimers of **1** and **2** are almost completely protected against quenching because of isolation from the bulk water environment. Both **1** and **2** show decreased and increased intensities for excimer and monomer emissions, respectively, upon guest binding. This observation indicates that they may be used as unique sensor systems, with which guest concentration can be correlated with pyrene excimer to monomer intensity ratio.

Two-guest inclusion of  $\gamma$ -cyclodextrin ( $\gamma$ -CD, cyclooctaamylose) is of current interest in cyclodextrin chemistry<sup>1</sup> and presents a new aspect in host–guest chemistry since the coinclusion phenomenon has rarely been observed with other hosts. This property of  $\gamma$ -CD enables it to be used as a molecular flask or container, in which two species can meet and react, and many applications might be possible on this basis as shown in some recent work, which reveals that  $\gamma$ -CD has remarkable promotion effects on

formation of excimers,<sup>1,2</sup> charge-transfer complexes,<sup>3</sup> and photodimers of anthracene derivatives.<sup>4</sup> On the other hand, the

(2) (a) Ueno, A.; Takahashi, K.; Osa, T. *J. Chem. Soc., Chem. Commun.* **1980**, 921. (b) Emert, J.; Kodali, D.; Catena, R. *J. Chem. Soc., Chem. Commun.* **1981**, 758. (c) Turro, N. J.; Okubo, T.; Weed, G. C. *Photochem. Photobiol.* **1982**, 35, 325. (d) Kobayashi, N.; Hino, Y.; Ueno, A.; Osa, T. *Bull. Chem. Soc. Jpn.* **1983**, 56, 1849. (e) Yellin, R. A.; Eaton, D. F. *J. Phys. Chem.* **1983**, 87, 5051. (f) Itoh, M.; Fujiwara, Y. *Bull. Chem. Soc. Jpn.* **1984**, 57, 2261. (g) Hamai, S. *Bull. Chem. Soc. Jpn.* **1986**, 59, 2979. (h) Eaton, D. *Tetrahedron* **1987**, 43, 1551.

(3) Kobayashi, N.; Saito, R.; Ueno, A.; Osa, T. *Makromol. Chem.* **1983**, 184, 837.

(1) Ueno, A.; Moriwaki, F.; Osa, T.; Hamada, F.; Murai, K. *J. Am. Chem. Soc.* **1988**, 110, 4323, and references therein.